# A Rational-Fraction Dispersion Model for Efficient Simulation of Dispersive Material in FDTD Method

Lin Han, Dong Zhou, Kang Li, *Member, IEEE*, Xun Li, *Senior Member, IEEE*, and Wei-Ping Huang, *Senior Member, IEEE*

***Abstract*—A novel rational-fraction dispersion model is proposed for simulation of optical properties of arbitrary linear dispersive media over a wide wavelength range. A generally applicable method is proposed for estimating the parameters of this model. It is demonstrated that the rational-fraction dispersion model can fit the relative permittivity data of a material accurately and efficiently in a wide wavelength range. The new model is implemented in the finite-difference time-domain method and is applied as a powerful and computationally efficient tool for simulating nano-particles of dispersive materials in a wide wavelength range of light.**

***Index Terms*—Dispersion, finite-difference method, nanoparticles, time-domain modeling.**

## I. Introduction

DISPERSIVE materials, such as semiconductors and metals, are widely used in optical devices. The finite-difference time-domain (FDTD) method [1] is one of the most common choices for simulating such devices in a wide frequency range. One of the most important advantages of the FDTD method is that the broadband response can be accurately obtained in only one simulation run [2]. Several simple phenomenological models, such as multi-pole Debye, Drude, and Lorentz models, have been widely adopted for modeling dispersive materials in the FDTD method [3]–[8]. To fit permittivity function of a given material accurately in a wide frequency range, a large number of poles are required in these models. Rakic and Djurisic used the Durde model with up to five Lorentzian terms to fit the permittivity functions of eleven metals [9]. Hao and Nordlander proposed an improved model consisting of four Lorentzian terms to fit dielectric data of gold and silver [10]. All the proposed multi-pole models archived good fit to the measure data. However, using a dispersion model with a large number of poles not only requires a lot of effort for modal parameter estimation but also dramatically increases the memory and computational costs of the FDTD method [11]. Jung and Teixeira extended the alternating-direction-implicit finite-difference time-domain (ADI-FDTD) method to model gold nanoparticles to improve computational performance in highly refined grids [12]. Lee *et al.* implemented the FDTD method on graphics processing unit (GPU) to save simulation time for plasmonics applications [13]. Han, Dutton and Fan proposed a complex-conjugate pole-residue pair model and implemented it in the FDTD method to increase the modeling efficiency [14], [15]. Etchegoin, Ru and Meyer proposed an analytical model with one Drude term and two critical points to modeling the optical properties of gold [16]. Okada and Cole proposed a modified effective permittivity model to analyse surface plasmons resonances on a coarse grid for saving memory and computation time [17].

A new model, referred to as the rational-fraction dispersion model (RFDM) is proposed in this paper for efficient modeling of arbitrary linear dispersive materials. The proposed model is more efficient than the conventional Debye, Drude, and Lorentz models because it has more degrees of freedom in parameter estimation. A feasible parameter estimation method is proposed for this model to fit the permittivity function efficiently and accurately. The rational-fraction dispersion model is implemented in the FDTD method. Both the memory and computational costs of the FDTD method for broadband dispersive material simulation could be reduced.

This paper is organized as follows. The RFDM and its numerical implementation in the FDTD method are described in Sections 2 and 3, respectively. The parameter estimation method is demonstrated in Section 4. The implemented FDTD method is verified by simulating a metal nanowire in Section 5.

## II. Rational-Fraction Dispersion Model

### A. The Rational-Fraction Dispersion Model in Frequency-Domain

Assuming the time harmonic dependence $\exp(j\omega t)$, the RFDM is proposed to describe the dispersive material's relative permittivity expressed by the rational fraction form as

$$\varepsilon_r(\omega) = \frac{\sum_{k=1}^{N} a_k (j\omega)^k}{\sum_{k=1}^{N} b_k (j\omega)^k} \tag{1}$$

Manuscript received February 22, 2012; revised March 17, 2012, April 09, 2012; accepted April 10, 2012. Date of publication April 19, 2012; date of current version May 07, 2012. This work was sponsored by NSERC Research Grant.

L. Han is with Department of Electrical and Computer Engineering, McMaster University, Hamilton, ON L8S 4L8, Canada (e-mail: han17@mcmaster.ca).

D. Zhou is now with Department of Electrical and Computer Engineering, McMaster University, Hamilton, ON L8S 4L8, Canada (e-mail: dongzh2000@hotmail.com).

K. Li is now with School of Information Science and Engineering, Shandong University, Jinan 250100, China (e-mail: kangli@sdu.edu.cn).

X. Li is with Department of Electrical and Computer Engineering, McMaster University, Hamilton, ON L8S 4L8, Canada and also with Wuhan National Laboratory for Optoelectronics, Wuhan 430074, China (e-mail:lixun@mcmaster.ca).

Wei-Ping Huang is now with Department of Electrical and Computer Engineering, McMaster University, Hamilton, ON, L8S 4L8, Canada (email: wphuang@univmail.cis.mcmaster.ca).

Digital Object Identifier 10.1109/JLT.2012.2195476

TABLE I
COEFFICIENTS OF DISPERSION MODELS

| $\varepsilon_r(\omega)$ | $L$ | $p_k$ | $r_k$ | $p_{k+1}$ | $r_{k+1}$ |
|---|---|---|---|---|---|
| Debye model $\varepsilon_\infty+\sum_{p=1}^{N_p}\frac{\Delta\varepsilon_p}{j\omega\gamma_p+1}$ | $N_p$ | $-1/\gamma_k$ | $\frac{\Delta\varepsilon_k}{\gamma_k}$ | - | - |
| Drude model $\varepsilon_\infty+\sum_{p=1}^{N_p}\frac{\omega_p^2}{-\omega^2+j\omega\gamma_p}$ | $2N_p$ | 0 | $\frac{\omega_p^2}{\gamma_p}$ | $-\gamma_p$ | $-\frac{\omega_p^2}{\gamma_p}$ |
| Lorentz model $\varepsilon_\infty+\sum_{p=1}^{N_p}\frac{\Delta\varepsilon_p\omega_p^2}{-\omega^2+2j\omega\gamma_p+\omega_p^2}$ | $N_p$ | $-\gamma_p-j\sqrt{\omega_p^2-\gamma_p^2}$ | $r_k=j\frac{\Delta\varepsilon_p\omega_p^2}{2\sqrt{\omega_p^2-\gamma_p^2}}$ $(\omega_p>\gamma_p)$ | - | - |
| Complex-conjugate pole-residue pair model $\varepsilon_\infty+\sum_{k=1}^{N_p}\left(\frac{r_k}{j\omega-p_k}+\frac{r_k^*}{j\omega-p_k^*}\right)$ | $N_p$ | Complex number | Complex number | - | - |
| Critical points model $\varepsilon_\infty+\sum_{p=1}^{N_p}A_p\omega_p\left(\frac{e^{j\phi_p}}{\omega_p-\omega-j\gamma_p}+\frac{e^{-j\phi_p}}{\omega_p+\omega+j\gamma_p}\right)$ | $N_p$ | $\gamma_p+j\omega_p$ | $-jA_p\omega_p e^{j\phi_p}$ | - | - |

where $a_k$ and $b_k$ are real numbers. The rational fraction form is the ratio of two polynomials $\sum_{k=1}^{N}a_k(j\omega)^k$ and $\sum_{k=1}^{N}b_k(j\omega)^k$, where the highest order of the denominator is the same as that of the numerator. The parameters $a_k$ and $b_k$ of the two polynomials can be estimated accurately and quickly by a rational approximation method and employed as a good initial guess for the material permittivity curve fitting method proposed in the later section of this paper. To be conveniently adopted by the FDTD method, the RFDM model is represented by its partial fraction expansion described by

$$\varepsilon_r(\omega)=\varepsilon_\infty+\sum_{k=1}^{L}\chi_k(\omega)$$
$$\chi_k(\omega)=\begin{cases}\dfrac{r_k}{j\omega-p_k}; & \text{if } p_k \text{ is real}\\ \dfrac{r_k}{j\omega-p_k}+\dfrac{r_k^*}{j\omega-p_k^*}; & \text{if } p_k \text{ is complex}\\ \sum_{u=1}^{U}\dfrac{r_{k,u}}{(j\omega-p_k)}; & \text{if } p_k \text{ is a multiple root}\end{cases}\tag{2}$$

where $\varepsilon_\infty$, $r_k$, and $p_k$ are the direct coefficient, residue, and pole, respectively. The partial fraction term $\chi_k(\omega)$is the frequency domain susceptibility function. It has three forms depending on the property of the pole $p_k$ : 1) a real fraction term with a real residue and a real pole when $p_k$ is a real number; 2) two complex fraction terms consist of complex conjugate residue and pole pairs when $p_k$ is a complex number; and 3) a summation of fraction terms which contains high order $(>1)$ of $j\omega$ when$p_k$ is a multiple root of the denominator $\sum_{k=1}^{N}b_k(j\omega)^k$. It is observed that the third expression of $P_k$ should be avoided in the parameter estimation procedure because the high order (the order of $j\omega$ is higher than one) partial fraction terms make it difficult to implement this model in the FDTD method. If there are $L_1$ real poles and $L_2$ complex conjugate pole pairs, the upper bound of the summation in (2) is $L=L_1+L_2$, and the total pole number is $N=L_1+2L_2$.

Table I shows the relationships of the RFDM with other dispersion models.

It shows that Debye, Drude, and Lorentz models are all special cases of RFDM with specified parameters. The RFDM treats the Debye, Drude, and Lorentz materials in a unified formulation, which simplifies the implementation of dispersion models in numerical simulation algorithms such as the FDTD method. It also shows that when $p_k$ is a complex number, the partial fraction form of the RFDM is the same as the complex-conjugate pole-residue pair model. The RFDM can also be converted to the critical points model by parameter substitution. The advantages of the RFDM, including the easy implementation in the FDTD method and the feasible parameter estimation process, will be demonstrated in the later sections.

### *B. The RDFM Oscillator*

Similar to the conventional phenomenological dispersion models, the RFDM describes the macroscopic susceptibility of a material. It is also very interesting to study the mechanism of the RFDM in the microscopic view. When $p_k$ is a real number, the susceptibility function has the same form as the Debye model. Therefore, in this case, the RFDM susceptibility has the same physical meaning as the Debye model which is the medium relaxation response of an ideal and non-interacting group of dipoles to an applied varying electric field. When $p_k$ is a complex number, each term of the susceptibility function can be reformed as

$$\chi_k(\omega)=\frac{(r_k+r_k^*)\,j\omega+(-r_kp_k^*-r_k^*p_k)}{-\omega^2-(p_k+p_k^*)\,j\omega+p_kp_k^*}\tag{3}$$

The corresponding polarization $\tilde{\mathbf{P}}_k(\omega)$ of this medium due to an applied electric field $\tilde{\mathbf{E}}(\omega)$ is described by

$$\tilde{\mathbf{P}}_k = \chi_k(\omega)\tilde{\mathbf{E}} = \frac{(r_k + r_k^*)\, j\omega + (-r_k p_k^* - r_k^* p_k)}{-\omega^2 - (p_k + p_k^*)\, j\omega + p_k p_k^*}\tilde{\mathbf{E}} \quad (4)$$

The macroscopic polarization $\tilde{\mathbf{P}}_k(\omega)$ of the medium is given by the summation over all dipole moments as

$$\tilde{\mathbf{P}}_k = \frac{N}{V}(-e\tilde{\mathbf{x}}) \quad (5)$$

where $e$, $N$, $V$, and $\tilde{\mathbf{x}}$ are the elementary charge, the number of dipoles, the volume of all the dipoles, and the displacement vector, respectively. Substituting (5) into (4) and after an obvious rearrangement, a new equation of the displacement vector is expressed as

$$\left[-\omega^2 - (p_k + p_k^*)\, j\omega + p_k p_k^*\right]\tilde{\mathbf{x}} = -\frac{V}{eN}\left[(r_k + r_k^*)\, j\omega + (-r_k p_k^* - r_k^* p_k)\right]\tilde{\mathbf{E}} \quad (6)$$

The corresponding time domain equation is obtained by inverse Fourier transforming and rearranging (6), yielding

$$\beta(-e)\frac{d\mathbf{E}}{dt} + \alpha(-e)\mathbf{E} + \delta\frac{d\mathbf{x}}{dt} - k\mathbf{x} = m_0\frac{d^2\mathbf{x}}{dt^2} \quad (7)$$

where

$$\begin{aligned}\alpha &= \frac{m_0 V}{e^2 N}\left(-r_k p_k^* - r_k^* p_k\right)\\ \beta &= \frac{m_0 V}{e^2 N}\left(r_k + r_k^*\right)\\ \delta &= m_0\left(p_k + p_k^*\right)\\ k &= m_0\left(p_k p_k^*\right)\end{aligned}$$

This formula is the motion equation of a system referred to as the "RFDM oscillator". It is noticed that this equation is very similar to the motion equation of a Lorentz oscillator of the Lorentz medium that describes the dispersive medium as a population of spring bounded electrons on nucleus. The motion equation of the Lorentz oscillator is given by

$$\alpha(-e)\mathbf{E} + \delta\frac{d\mathbf{x}}{dt} - k\mathbf{x} = m_0\frac{d^2\mathbf{x}}{dt^2} \quad (8)$$

where

$$\begin{aligned}\alpha &= \frac{\Delta\varepsilon_p\omega_p^2 V m_0}{e^2 N} = 1\\ \delta &= -2m_0\gamma_p\\ k &= m_0\omega_p^2\end{aligned}$$

Comparing (7) with (8), it is easy to find that the only difference of the two equations is that (7) has an extra term $\beta(-e)(d\mathbf{E})/(dt)$ while (8) does not. Therefore, in this case when $p_k$ is a complex number, the RFDM describes a population of RFDM oscillators moving under the action of the instantaneous electric filed $\mathbf{E}$, as well as its derivative $d\mathbf{E}/dt$. From the mathematical point of view, the RFDM oscillator gives more degrees of freedom compared with the Lorentz oscillator. If the RFDM's parameter $r_k$ is purely imaginary, the coefficient $\beta$ in (7) becomes zero. In this case, the RFDM oscillator degenerates to the Lorentz oscillator.

### C. Analysis of the RFDM in Time Domain

To study properties of the RFDM in time domain, the inverse Fourier transformation is performed on the frequency domain susceptibility function $\chi_k(\omega)$ defined in (2). If $p_k$ is a real number, the time domain susceptibility is expressed by

$$\chi_k(t) = r_k e^{p_k^t} U(t) \quad (9)$$

where $U(t)$ is the unit step function. It shows that when $p_k > 0$, the susceptibility is exponentially growing with time, which contradicts the phenomenon that the lightwave is decaying when propagating in lossy materials such as metals and semiconductors. Thus, the parameter $p_k$ should not be greater than zero when modeling lossy materials using this model. If $p_k$ is a complex number, the frequency domain susceptibility can be reformed as

$$\chi_k(\omega) = \frac{(-r_k p_k^* - r_k^* p_k)}{-\omega^2 - (p_k + p_k^*)\, j\omega + p_k p_k^*} + j\omega\frac{(r_k + r_k^*)}{-\omega^2 - (p_k + p_k^*)\, j\omega + p_k p_k^*} \quad (10)$$

The time domain susceptibility is obtained by taking the inverse Fourier transformation, as expressed by

$$\chi_k(t) = \zeta_k e^{-\alpha_k^t}\sin(\kappa_k t)U(t) + \frac{d}{dt}\left[\xi_k e^{-\alpha_k^t}\sin(\kappa_k t)U(t)\right] \quad (11)$$

where

$$\begin{aligned}\alpha_k &= -\frac{p_k + p_k^*}{2} = -\mathrm{Re}(p_k)\\ \kappa_k &= \sqrt{p_k p_k^* - \alpha_k^2}\\ \zeta_k &= \frac{-r_k p_k^* - r_k^* p_k}{\kappa_k}\\ \xi_k &= \frac{r_k + r_k^*}{\kappa_k}\end{aligned}$$

It is noticed that when the real part of $p_k$ is positive ($\mathrm{Re}(p_k) > 0$), the parameter $\alpha_k$ is negative ($\alpha_k < 0$). The time domain susceptibility $\chi_k(t)$ will grow exponentially with time, which contradicts the property of the lossy materials. A natural conclusion from the above analysis is that the real part of the pole parameter$p_k$ must be no bigger than zero ($\mathrm{Re}(p_k) \le 0$) when using the RFDM modeling lossy dispersive materials.

## III. Implementation of the RFDM in the FDTD Method

The RFDM can be easily and efficiently implemented in the FDTD method with an auxiliary differential equation (ADE) scheme. In Maxwell's equations, Ampere's law in frequency domain is expressed by

$$j\omega\varepsilon_0\varepsilon_\infty\tilde{\mathbf{E}} + \sigma\tilde{\mathbf{E}} + \sum_{k=1}^{L}\tilde{\mathbf{J}}_k = \nabla\times\tilde{\mathbf{H}} \quad (12)$$

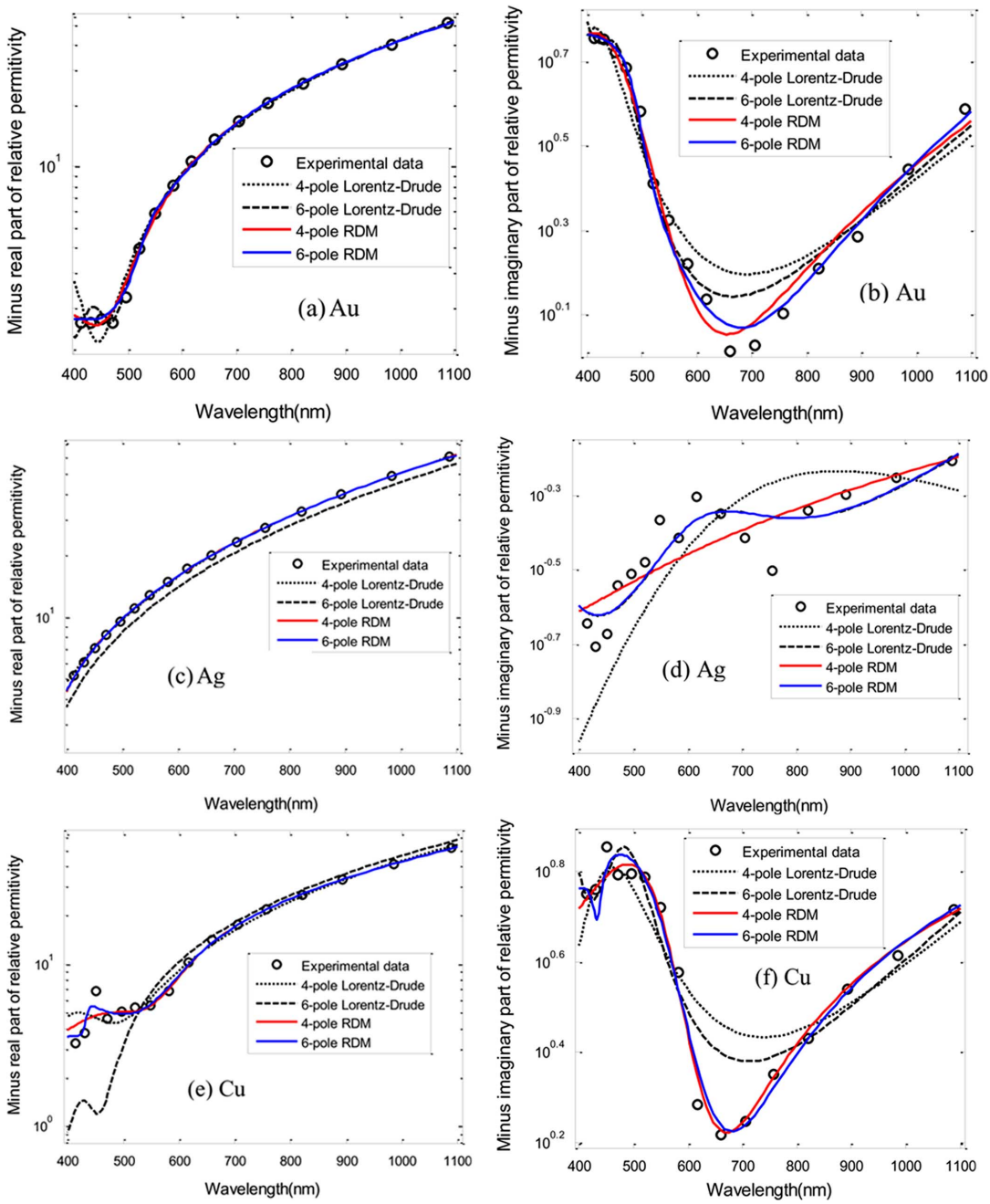


Fig. 1. (a) Real (minus) and (b) imaginary (minus) parts of the permittivity function of Au; (c) real (minus) and (d) imaginary (minus) parts of the permittivity function of Ag; (e) real (minus) and (f) imaginary(minus) parts of the permittivity function of Cu: the black circles are experimental data taken from [24]; the black dot and dashed lines are fitting curves with 4-pole Lorentz-Drude model (1 Drude pole pair and 1 Lorentz pole pair) and 6-pole Lorentz-Drude model (1 Drude pole pair and 2 Lorentz pole pairs), respectively; the solid red and blue lines are the fitting curves with 4-pole RFDM and 6-pole RFDM, respectively.

where $\tilde{\mathbf{J}}_k$ is the polarization current related with each term in the summation of the RFDM, defined by

$$\tilde{\mathbf{J}}_k = j\omega\varepsilon_0\tilde{\mathbf{E}}\begin{cases}\dfrac{r_k}{j\omega - p_k}; & \text{if } p_k \text{ is real}\\ \dfrac{r_k}{j\omega - p_k} + \dfrac{r_k^*}{j\omega - p_k^*}; & \text{if } p_k \text{ is complex}\end{cases} \tag{13}$$

As mentioned previously, the multiple-root $p_k$ is avoided in the parameter estimation procedure, so that it is not concerned with the difficult implementation of polarization current in the multiple-root $p_k$ case.

If $p_k$ is real, $r_k$ is also real, then the time-domain polarization current is real and given by

$$\frac{\partial \mathbf{J}_k}{\partial t} - p_k\mathbf{J}_k = r_k\varepsilon_0\frac{\partial \mathbf{E}}{\partial t} \tag{14}$$

If $p_k$ is complex, $r_k$ is also complex. The time-domain polarization current has two parts $\mathbf{J}_k$ and$\mathbf{J'}_k$, corresponding to the

two complex poles in (13). The two polarization currents are all complex and given by

$$\frac{\partial \mathbf{J}_k}{\partial t} - p_k \mathbf{J}_k = r_k \varepsilon_0 \frac{\partial \mathbf{E}}{\partial t} \tag{15}$$

$$\frac{\partial \mathbf{J'}_k}{\partial t} - p_k^* \mathbf{J'}_k = r_p^* \varepsilon_0 \frac{\partial \mathbf{E}}{\partial t} \tag{16}$$

Because $\mathbf{E}(t)$ is real, if the initial values for the two polarization current are the same, the two parts are mutual complex conjugate, i.e., $\mathbf{J'}_k = \mathbf{J}_k^*$ [14]. Only one complex equation, either (15) or (16), needs to be computed in the FDTD calculation. In the following derivation, (15) is employed. Therefore, when $p_k$ is complex, the real part of the time domain polarization current is $\mathrm{Re}[\mathcal{F}^{-1}(\tilde{\mathbf{J}}_k)] = 2\mathrm{Re}(\mathbf{J}_k)$. By applying the inverse Fourier transform on both sides of (12), the time domain Ampere's curl equation is obtained as

$$\varepsilon_0 \varepsilon_\infty \frac{\partial}{\partial t}\mathbf{E} + \sigma \mathbf{E} + \sum_{k=1}^{L} m\mathrm{Re}(\mathbf{J}_k) = \nabla \times \mathbf{H} \tag{17}$$

where $m = 1$if$p_k$ is real; $m = 2$ if $p_k$ is complex. The time domain polarization current equation and Ampere's curl equation are combined together and discretized in the explicit FDTD scheme, yielding

$$\begin{aligned}\mathbf{E}|^{n+1/2} &= C_a \mathbf{E}|^{n-1/2} \\ &\quad + C_b \left[ \nabla \times \mathbf{H}|^n - \mathrm{Re}\left( \sum_{k=1}^{L} \frac{m}{2}(1+k_p)\mathbf{J}_k|^{n-1/2} \right) \right]\end{aligned} \tag{18}$$

$$\mathbf{J}_k|^{n+1/2} = k_k \mathbf{J}_k|^{n-1/2} + \beta_k \left( \frac{\mathbf{E}|^{n+1/2} - \mathbf{E}|^{n-1/2}}{\Delta t} \right) \tag{19}$$

where

$$\begin{aligned} k_k &= \frac{2 + p_k \Delta t}{2 - p_k \Delta t}; \quad \beta_k = \frac{2 r_k \varepsilon_0 \Delta t}{2 - p_k \Delta t} \\ C_a &= \frac{2\varepsilon_0\varepsilon_\infty - \sigma\Delta t + \mathrm{Re}\sum_{k=1}^{L}(m\beta_k)}{2\varepsilon_0\varepsilon_\infty + \sigma\Delta t + \mathrm{Re}\sum_{k=1}^{L}(m\beta_k)} \\ C_b &= \frac{2\Delta t}{2\varepsilon_0\varepsilon_\infty + \sigma\Delta t + \mathrm{Re}\sum_{k=1}^{L}(m\beta_k)} \\ m &= \begin{cases} 1; & \text{if } p_k \text{ is real} \\ 2; & \text{if } p_k \text{ is complex} \end{cases} \end{aligned} \tag{20}$$

The discretization of the magnetic field $\mathbf{H}|^{n+1}$ is the same as it is in the standard FDTD algorithm [1]. This is an efficient implementation of the RFDM in the FDTD method. With the same number of poles, the RFDM takes no additional memory and computational costs in the FDTD method for updating the auxiliary equations of the polarization currents compared with the conventional dispersion models such as multi-pole

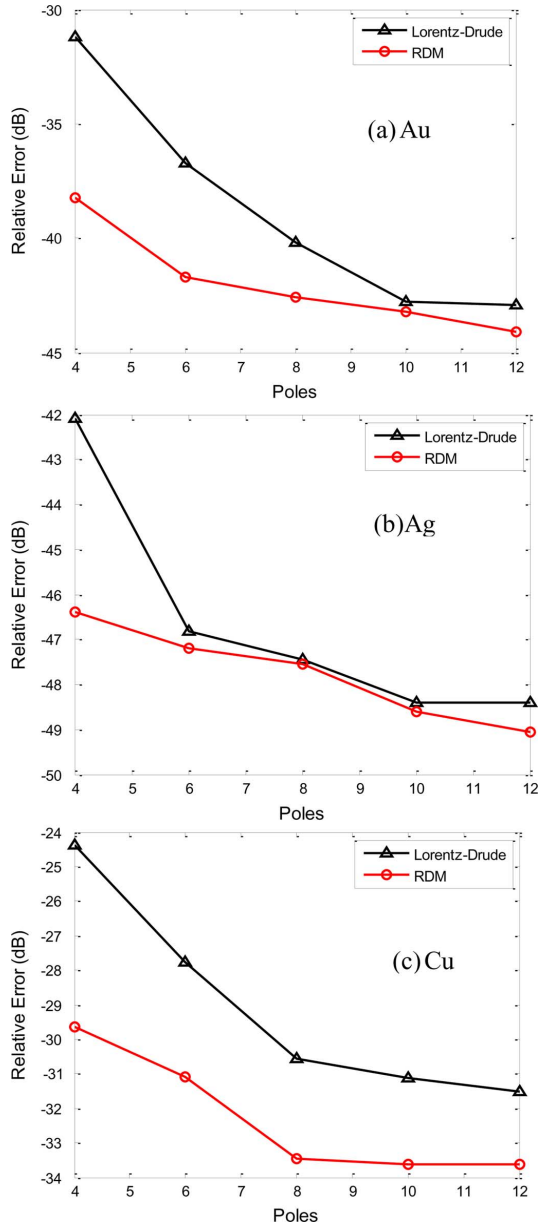


Fig. 2. Relative errors of modeled permittivity of (a) Au, (b) Ag, and (C) Cu versus the number of poles in the models: the black line is the relative error of the Lorentz-Drude model, and the red line is the relative error of the RFDM.

Lorentz-Drude model. However, the RFDM has more degrees of freedom in fitting a permittivity function in the parameter estimation process. Thus, the implementation of the RFDM in the FDTD method is far more computationally efficient compared with those of Lorentz-Drude model. This implementation is much easier than the critical points model implementation with recursive convolution method [18] or ADE method [19] in which the Drude and the critical point expressions are implemented separately with different derivations.

## IV. Parameter Estimation of the RFDM

The RFDM is an analytical function describing the relative permittivity of a dispersive material. To fit a given relative permittivity curve accurately and quickly, a feasible parameter estimation procedure is highly demanded to obtain a good

TABLE II
VALUES OF THE PARAMETERS FOR THE LORENTZ-DRUDE MODEL (AU)

| Parameters | 1 Drude 1 Lorentz | 1 Drude 2 Lorentz | 1 Drude 3 Lorentz | 1 Drude 4 Lorentz | 1 Drude 5 Lorentz |
|---|---|---|---|---|---|
| $\varepsilon_\infty$ | 6.069 | 5.035 | 2.541 | 1.000 | 1.000 |
| $\omega_D$ (eV) | 8.829 | 8.739 | 8.646 | 8.229 | 8.225 |
| $\gamma_D$ (eV) | 5.617e-2 | 6.274e-2 | 6.596-2 | 1.035e-7 | 3.539-8 |
| $\Delta\varepsilon_1$ | 1.930 | 7.360e-1 | 8.834e-1 | 1.190 | 5.324e-1 |
| $\omega_1$ (eV) | 3.038 | 2.750 | 3.075 | 3.088 | 2.678 |
| $\gamma_1$ (eV) | 5.034e-1 | 2.858e-1 | 3.053e-1 | 3.870e-1 | 2.635e-1 |
| $\Delta\varepsilon_2$ | - | 1.309 | 1.910 | 2.901 | 2.896 |
| $\omega_2$ (eV) | - | 3.316 | 3.932 | 4.285 | 4.280 |
| $\gamma_2$ (eV) | - | 3.494e-1 | 5.859e-9 | 1.276e-9 | 1.892e-7 |
| $\Delta\varepsilon_3$ | - | - | 6.520e-1 | 5.288e-1 | 1.184 |
| $\omega_3$ (eV) | - | - | 2.688 | 2.677 | 3.088 |
| $\gamma_3$ (eV) | - | - | 2.686e-1 | 2.629e-1 | 3.857e-1 |
| $\Delta\varepsilon_4$ | - | - | - | 9.679 | 9.799 |
| $\omega_4$ (eV) | - | - | - | 7.594e-1 | 7.573e-1 |
| $\gamma_4$ (eV) | - | - | - | 2.420e-1 | 2.412e-1 |
| $\Delta\varepsilon_5$ | - | - | - | - | 1.109e-6 |
| $\omega_5$ (eV) | - | - | - | - | 2.736e-1 |
| $\gamma_5$ (eV) | - | - | - | - | 8.050e-2 |

initial guess as a starting point and locate a good approximation to the global optimum for any linear dispersive material. The advantage of the rational fraction form of the RFDM in (1) is that a very good initial guess of parameters $a_k$ and $b_k$ can be quickly obtained using the rational approximation method [20]–[22]. After that, the initial values of the residues $r_k$, poles $p_k$, and direct coefficient $\varepsilon_\infty$ are obtained from the parameters $a_k$ and $b_k$ by converting the RFDM from the rational fraction form in (1) to the partial fraction form in (2). The conversion process is very fast. It takes very limited computational effort which could almost be neglected. Note that the multiple root$p_k$ in (2) should be avoided because the higher order partial fraction terms make it difficult to implement this model in the FDTD method. Fortunately, the multiple root case seldom shows up. In case it happens, one could vary the wavelength range a little bit and re-do the parameter estimation until it disappears. Finally, the initial values are employed in a simulated annealing algorithm [23] to find the optimized values of parameters $\varepsilon_\infty$, $p_k$ and $r_k$. In the simulated annealing optimization, the relative error of the modeled permittivity to the experimental data defined in (22) is used as the objective function. A relative error small enough to satisfy the application's accuracy requirement or a maximum number of consecutive rejections can be set as the stop criterions. The simulated annealing optimization is time consuming. Typically, it takes several to tens of minutes to produce the optimized values depending on the number of the model parameters and the wavelength range of the permittivity spectrum one wants to fit. Fortunately, the model parameters are "lifelong" values for each material in a specific wavelength range. Once the model parameters of a material for one wavelength range are obtained in the optimization, they can be used in many FDTD simulations of different applications with this material involved. The parameters have not to be estimated before every FDTD simulation. Only when a new wavelength range in a simulation is demanded and the parameters have not been estimated for it, the optimization procedure should be processed and the produced parameters can be saved for the present and future use in the FDTD method.

The high efficiency of the RFDM is demonstrated by modeling metal materials Au (gold), Ag (silver) and Cu (copper) in a wide wavelength range from 400 to 1100 nm. The measured relative permittivity of the three metals [24] is fitted by four dispersion models: the 4-pole Lorentz-Drude model (1 Drude pole pair and 1 Lorentz pole pair), the 6-pole Lorentz-Drude model (1 Drude pole pair and 2 Lorentz pole pairs), the RFDM with 4 poles, and the RFDM with 6 poles. The Lorentz-Drude model is expressed by the equation

$$\varepsilon_r(\omega) = \varepsilon_\infty + \frac{\omega_D^2}{-\omega^2 + j\omega\gamma_D} + \sum_{l=1}^{N_L} \frac{\Delta\varepsilon_l \omega_l^2}{-\omega^2 + 2j\omega\gamma_l + \omega_l^2} \quad (21)$$

where the numbers of Drude, and Lorentz pole pairs are one, and $N_L$, respectively.

In the curve fitting procedure using the Lorentz-Drude model, the initial parameters cannot be obtained by using the mathematical methods for the RFDM of (1). Instead, the initial parameters are obtained from literatures [3], [7], [9]. Once the initial values are obtained, the same stimulated annealing algorithm is used to refine the parameters as we did in the RFDM curve fitting. The advantage of using the modal of (1) for RFDM is that a good initial guess could be estimated very quickly for new materials

TABLE III
VALUES OF THE PARAMETERS FOR THE RFDM (AU)

| Parameters | 4-pole RFDM | 6-pole RFDM | 8-pole RFDM | 10-pole RFDM | 12-pole RFDM |
|---|---|---|---|---|---|
| $\varepsilon_\infty$ | 2.988 | 1.000 | 1.366 | 1.000 | 1.000 |
| $p_1$ (eV) | -1.745e-2 -1.079e-2i | -2.356e-2 -8.549e-2i | -3.719e-10 -9.473e-2i | -1.484e-9 -1.364e-1i | -4.216e-9 -1.054e-1i |
| $r_1$ (eV) | 1.464 +3.397e+3i | 1.533 +4.210e+2i | 2.308 +3.710e+2i | 8.279e-1 +2.603e+2i | -2.018 +3.430e+2i |
| $p_2$ (eV) | -1.745e-2 +1.079e-2i | -2.356e-2 +8.549e-2i | -3.719e-10 +9.472e-2i | -1.484e-9 +1.364e-1i | -4.216e-9 +1.054e-1i |
| $r_2$ (eV) | 1.464 -3.397e+3i | 1.533 -4.210e+2i | 2.308 -3.710e+2i | 8.279e-1 -2.603e+2i | -2.018 -3.430e+2i |
| $p_3$ (eV) | -6.805e-1 -2.602i | -2.329e-1 -2.521i | -1.716e-10 -1.037i | -9.667e-9 -9.334e-1i | -6.634e-10 -7.769e-1i |
| $r_3$ (eV) | 3.686 +1.660i | 3.873e-1 +3.146e-2i | 1.354e-1 +7.042e-2i | 5.839e-1 +9.971e-2i | 2.251 +2.487e-1i |
| $p_4$ (eV) | -6.805e-1 +2.602i | -2.329e-1 +2.521i | -1.716e-10 +1.037i | -9.667e-9 +9.334e-1i | -6.634e-10 +7.769e-1i |
| $r_4$ (eV) | 3.686 -1.660i | 3.873e-1 -3.146e-2i | 1.354e-1 -7.042e-2i | 5.839e-1 -9.971e-2i | 2.251 -2.487e-1i |
| $p_5$ (eV) | - | -1.186 -2.390i | -2.127e-1 -2.508i | -1.366e-1-2.461i | -2.254e-1 -2.335i |
| $r_5$ (eV) | - | 7.246 +1.796e-1i | 3.156e-1 -2.150e-2i | 8.992e-2 -6.297e-2i | -4.081e-1 +6.295e-2i |
| $p_6$ (eV) | - | -1.186 +2.390i | -2.127e-1 +2.508i | -1.366e-1 +2.461i | -2.254e-1 +2.335i |
| $r_6$ (eV) | - | 7.246 -1.796e-1i | 3.156e-1 +2.150e-2i | 8.992e-2 +6.297e-2i | -4.081e-1 -6.295e-2i |
| $p_7$ (eV) | - | - | -1.040 -2.358i | -7.099e-1 -2.564i | -3.450e-1 -2.455i |
| $r_7$ (eV) | - | - | 6.141 -2.946e-1i | 3.408 +1.755i | 1.585 +3.928e-1i |
| $p_8$ (eV) | - | - | -1.040 +2.358i | -7.099e-1 +2.564i | -3.450e-1 +2.455i |
| $r_8$ (eV) | - | - | 6.141 +2.946e-1i | 3.408 -1.755i | 1.585 -3.928e-1i |
| $p_9$ (eV) | - | - | - | -8.789e-10 -4.533i | -3.486e-1 -3.661i |
| $r_9$ (eV) | - | - | - | -2.085e-1 +3.024i | -9.571 +2.662i |
| $p_{10}$ (eV) | - | - | - | -8.789e-10 +4.533i | -3.486e-1 +3.661i |
| $r_{10}$ (eV) | - | - | - | -2.085e-1 -3.024i | -9.571 -2.662i |
| $p_{11}$ (eV) | - | - | - | - | -4.312e-10 -3.815i |
| $r_{11}$ (eV) | - | - | - | - | 7.567 +5.354i |
| $p_{12}$ (eV) | - | - | - | - | -4.312e-10 +3.815i |
| $r_{12}$ (eV) | - | - | - | - | 7.567 -5.354i |

by using the mathematical methods described in existing literatures such as [20]–[22].

As it is shown in Fig. 1, both the Lorentz-Drude model and the RFDM achieve better accuracy with more number of poles. However, the RFDM overwhelms the Lorentz-Drude model with significant improvement of accuracy under the same number of poles. Moreover, for some materials such as Au and Cu, the RFDM with 4 poles fits the experimental data in a higher accuracy than the 6-pole Lorentz-Drude model, while having lower computational cost. The RFDM with 6 poles performs a more accurate fit than the 6-pole Lorentz-Drude model, while having the same computational cost.

To demonstrate the advantages of the RFDM in terms of the modeling accuracy, a convergence test of the RFDM is performed on the three metal materials Au, Ag and Cu. The convergence of the RFDM is studied by measuring the relative errors of the modeled permittivity with increasing the number of

TABLE IV
COMPUTATIONAL COSTS AND RELATIVE ERRORS OF DIFFERENT FDTD SCHEMES

| | Scheme 1 (1 Drude pole pair and 2 Lorentz pole pairs) | Scheme 2 (4 RFDM poles) | Scheme 3 (6 RFDM poles) |
|---|---|---|---|
| Memory (mega-byte) | 6.600 | 5.872 | 6.604 |
| Computation time (second) | 694.58 | 599.26 | 702.04 |
| Relative error (dB) (Extinction cross-section) | -23.97 | -25.31 | -26.04 |

poles. The relative error of the modeled permittivity to the experimental data is defined by

$$e_{\text{rel}} = \frac{\sqrt{\sum_{i=1}^{N} \left|\varepsilon^{\text{exp}}(\omega_i) - \varepsilon(\omega_i)\right|^2}}{\sqrt{\sum_{i=1}^{N} \left|\varepsilon^{\text{exp}}(\omega_i)\right|^2}} \tag{22}$$

Fig. 2 depicts the relative errors of the RFDM and the Lorentz-Drude mode in modeling the permittivity of the metal materials Au, Ag and Cu. It shows that when increasing the number of poles, both the RFDM and the Lorentz-Drude model reduce the relative errors. However, the RFDM model converges faster than the Lorentz-Drude model. The parameters of the Lorentz-Drude model and the RFDM model for modeling material Au are listed in Tables II and III, respectively.

## V. FDTD SIMULATION OF THE METAL NANO-PARTICLE

The FDTD method is a rigorous numerical tool which has been widely employed in simulating nano-particle problems [25], [26]. However, it is extremely memory and time consuming when dealing with metal nano-structures in the wavelength range of light because of two reasons: 1) the small feature size of the structure requires very fine meshes and time steps; and 2) the complicated dispersion property dramatically increases the implementation complexity and computational cost. Therefore, it is strongly desired to have a simulation tool, which can accurately model the wide band dispersion properties, yet taking an affordable computation effort. The RFDM is implemented in 2-D and 3-D FDTD methods for simulating of nano-structures.

### *A. Simulation of Nano-Wire With 2-D FDTD Method*

To examine the efficiency of the RFDM with different numbers of poles, the light wave scattering phenomenon of an Au nano-wire with 40 nm diameter surrounded by air is simulated by the 2-D FDTD method with the RFDM in a wide wavelength range from 400 to 1100 nm. The CPML [27] is employed to truncate the computation window. A uniform mesh size of 0.5 nm is employed and 20 000 time steps are performed. Fig. 3 shows the cross section curves calculated using the analytical solution, the FDTD method with 1 Drude pole pair and 2 Lorentz pole pairs(scheme 1), the FDTD method with the 4-pole RFDM(scheme 2), and the FDTD method with the 6-pole RFDM(scheme 3), respectively. Table IV lists the memory and computational costs of different FDTD schemes, as well as the relative errors of the extinction cross section compared with the analytical solution. It shows that compared with the conventional Lorentz-Drude model, the FDTD method with the 4-pole RFDM achieves a smaller relative error ($-25.31$ dB versus $-23.97$ dB) while taking less computational effort (599.26 sec. versus 694.58 sec.), and the FDTD method with the 6-pole achieves even better accuracy ($-26.31$ dB versus $-23.97$ dB) yet maintaining a comparable computational cost (702.04 sec. versus 695.58 sec.). In this application, only a partial space is occupied by dispersive material (metal cylindrical surrounded by air). In some applications where dispersive materials are dominant, more memory and computation time could be saved. If lower accuracy is acceptable, 2-pole or 3-pole RFDM can be used, then the computational effort would be further reduced.

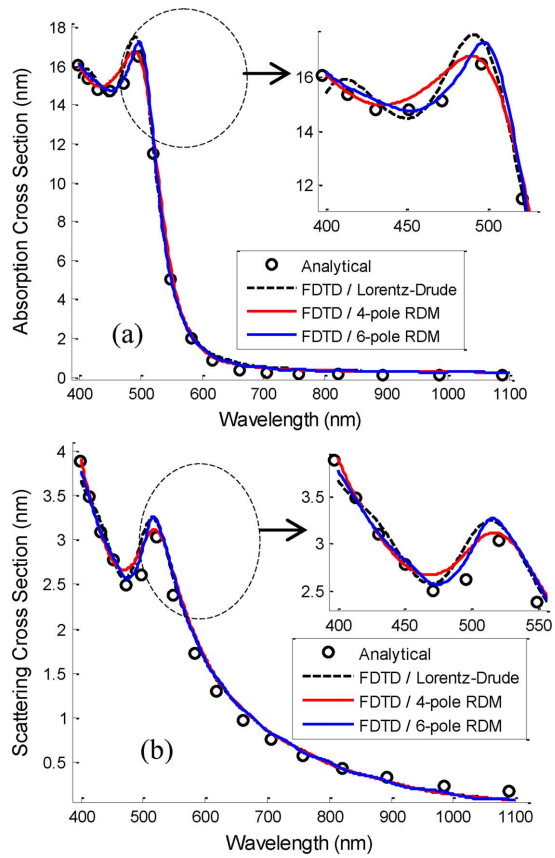


Fig. 3. (a) Absorption cross section (b) Scattering cross-section: the black circles are analytical solution with experimental data [24]; the black dashed line is the FDTD solution with 1 Drude pole pair and 2 Lorentz pole pairs; the solid red and blue lines are the FDTD solutions with 4-pole RFDM and 6-pole RFDM, respectively.

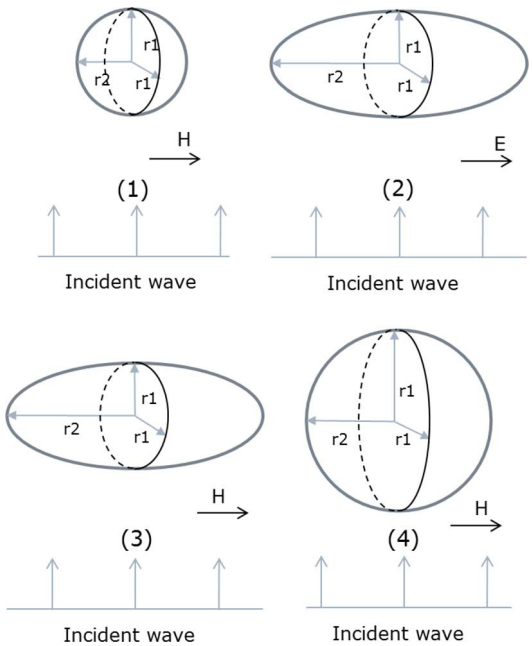


Fig. 4. Four configurations for single gold nano-ellipsoid simulation: (a) a nano-ellipsoid with all radii equal to 10nm; (b) a gold nano-ellipsoid with a longer radius $r2 = 20$ nm and two shorter radii $r1 = 20$ nm illuminated by a plane wave with electric field polarized parallel to the longer radius; (c) a gold nano-ellipsoid with a longer radius $r2 = 20$ nm and two shorter radii $r1 = 20$ nm illuminated by a plane wave with magnetic field polarized parallel to the longer radius; (d) a nano-ellipsoid with all radii equal to 20 nm.

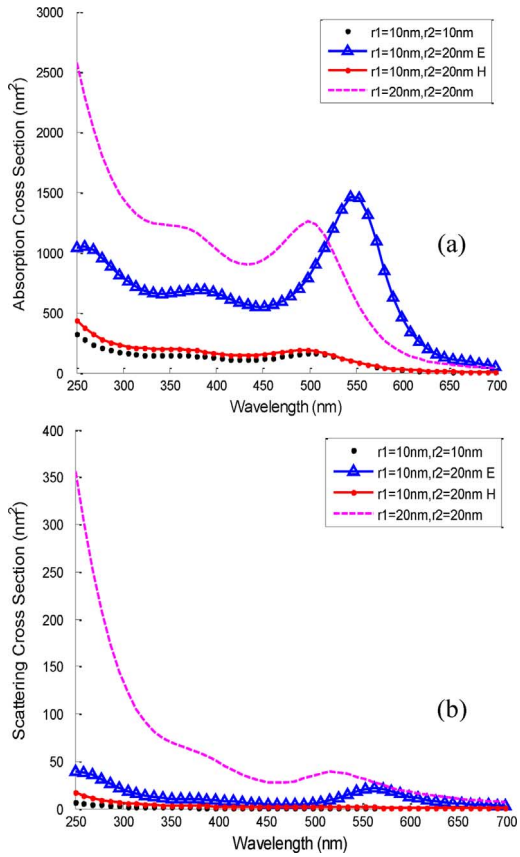


Fig. 5. Absorption (a) and scattering (b) cross section spectra of gold nano-particles with different radii and incident wave polarizations: black dots are results for configuration (1); blue triangle lines are results for configuration (2); red dot lines are results for configuration (3); purple dashed lines are results for configuration (4).

### *B. Simulation of Nano-Particle With 3-D FDTD Method*

The RFDM is implemented in the 3-D FDTD method and employed to simulate the optical properties of a single gold nano-ellipsoid [21] with different configurations regarding the radius length and incident wave polarization. Four different configurations are shown in Fig. 4(1), (2), (3), and (4), respectively. In configuration (1), the lengths of the three radii of the nano-ellipsoid are all 10nm, thus the particle is a nano-sphere. In configuration (2), the gold nano-ellipsoid has a longer radius $r2 = 20$ nm and two shorter radii $r1 = 20$ nm. It is illuminated by a plane wave propagating perpendicular to the longer radius and electric field polarized parallel to the longer radius. In configuration (3), the nano-ellipsoid has the same geometry of configuration (2) but the magnetic field instead of the electric field is polarized parallel to the longer radius. In configuration (4), the particle is a nano-sphere with a 20 nm radius. The nano-particle is surrounded by air in all the configurations. In the 3-D FDTD simulation, a uniform mesh size of 1.0 nm is employed and 30 000 time steps are performed. The 4-pole RFDM is used for modeling the gold material. The absorption and scattering cross section spectra of the single nano-ellipsoid with above four different configurations are compared and depicted in In Fig. 5(a) and (b), respectively. Comparing the black dots for configuration (1) and the red dot-line for configuration (3) in Fig. 5(a), one can realize that although the radius of the nano-particle parallel to the magnetic field polarization is doubled, the absorption cross section is not enlarged very much. However, when the radius parallel to the electric field polarization is doubled, the absorption is dramatically enhanced as shown in Fig. 5(a) by comparing the black dots for configuration (1) and the blue triangle-line for configuration (2). From above comparisons, one can conclude that the absorption effect is mainly affected by the length of the radius which is parallel to the direction of the electric field polarization. The scattering cross section is mainly determined by the particle size as shown in Fig. 5(b).

## VI. Conclusion

The RFDM with a feasible parameter estimation method is proposed in this paper. The new model is proven to be more efficient in terms of memory and computational costs in modeling dispersive materials in comparison with conventional phenomenological models. The RFDM is implemented in the FDTD method, forming a powerful and efficient tool for simulating broadband optical phenomena of nano-particles with dispersive materials.

## Acknowledgment

The authors would like to express their gratitude to Dr. Y. Xi and Dr. L. Deng for useful discussions regarding the properties of optical devices, and Dr. F. Kong for insightful discussions regarding the FDTD algorithms.

## References

[1] A. Taflove and S. Hagness, , Wiley, Ed., *Computational Electrodynamics: The Finite-Difference Time-Domain Method*, 3rd ed. Norwood, MA: Artech House, 2005.

[2] S. H. Chang, S. Gray, and G. Schatz, "Surface plasmon generation and light transmission by isolated nanoholes and arrays of nanoholes in thin metal films," *Opt. Exp.*, vol. 13, pp. 3150–3165, 2005.
[3] T. W. Lee and S. Gray, "Subwavelength light bending by metal slit structures," *Opt. Exp.*, vol. 13, pp. 9652–9659, 2005.
[4] A. Vial, A. S. Grimault, D. Macías, D. Barchiesi, and M. L. de la Chapelle, "Improved analytical fit of gold dispersion: Application to the modeling of extinction spectra with a finite-difference time-domain method," *Phys. Rev. B*, vol. 71, p. 085416, 2005.
[5] D. F. Kelley and R. J. Luebbers, "Piecewise linear recursive convolution for dispersive media using FDTD," *IEEE Trans. Antennas Propag.*, vol. 44, no. 6, pp. 792–797, Jun. 1996.
[6] T. Laroche and C. Girard, "Near-field optical properties of single plasmonic nanowires," *Appl. Phys. Lett.*, vol. 89, p. 233119, 2006.
[7] J. M. McMahon, J. Henzie, T. W. Odom, G. C. Schatz, and S. K. Gray, "Tailoring the sensing capabilities of nanohole arrays in gold films with Rayleigh anomaly-surface plasmon polaritons," *Opt. Exp.*, vol. 15, pp. 18119–18129, 2007.
[8] S. K. Gray and T. Kupka, "Propagation of light in metallic nanowire arrays: Finite-difference time-domain studies of silver cylinders," *Phys. Rev. B*, vol. 68, p. 045415, 2003.
[9] A. D. Rakic, A. B. Djurisic, J. M. Elazar, and M. L. Majewski, "Optical properties of metallic films for vertical-cavity optoelectronic devices," *Appl. Opt.*, vol. 37, pp. 5271–5283, 1998.
[10] F. Hao and P. Nordlander, "Efficient dielectric function for FDTD simulation of the optical properties of silver and gold nanoparticles," *Phys. Chem. Lett.*, vol. 446, pp. 115–118, 2007.
[11] A. Vial and T. Laroche, "Comparison of gold and silver dispersion laws suitable for FDTD simulations," *Appli. Phys. B: Lasers Opt.*, vol. 93, pp. 139–143, 2008.
[12] K. Y. Jung and F. L. Teixeira, "Multispecies ADI-FDTD algorithm for nanoscale three-dimensional photonic metallic structures," *IEEE Photon. Technol. Lett.*, vol. 19, no. 8, pp. 586–588, Apr. 2007.
[13] K. H. Lee, I. Ahmed, R. S. M. Goh, E. H. Khoo, E. P. Li, and T. G. G. Hung, "Implementation of the FDTD method based on Lorentz-Drude dispersive model on GPU for plasmonics applications," *Progr. Electromagn. Res.*, vol. 116, pp. 441–456, 2011.
[14] M. Han, R. W. Dutton, and S. Fan, "Model dispersive media in finite-difference time-domain method with complex-conjugate pole-residue pairs," *IEEE Microw. Wireless Comp. Lett.*, vol. 16, pp. 119–121, 2006.
[15] I. Udagedara, M. Premaratne, I. D. Rukhlenko, H. T. Hattori, and G. P. Agrawal, "Unified perfectly matched layer for finite-difference time-domain modeling of dispersive optical materials," *Opt. Exp.*, vol. 17, pp. 21179–21190, 2009.
[16] P. Etchegoin, E. Le Ru, and M. Meyer, "An analytic model for the optical properties of gold," *J. Chem. Phys.*, vol. 125, p. 164705, 2006.
[17] N. Okada and J. B. Cole, "Effective permittivity for FDTD calculation of plasmonic materials," *Micromachines*, vol. 3, pp. 168–179, 2012.
[18] A. Vial, "Implementation of the critical points model in the recursive convolution method for modelling dispersive media with the finite-difference time domain method," *J. Opt. A: Pure Appl. Opt.*, vol. 9, p. 745, 2007.
[19] M. Hamidi, F. Baida, A. Belkhir, and O. Lamrous, "Implementation of the critical points model in a SFM-FDTD code working in oblique incidence," *J. Phys. D Appl. Phys.*, vol. 44, p. 245101, 2011.
[20] B. Gustavsen and A. Semlyen, "Rational approximation of frequency domain responses by vector fitting," *IEEE Trans. Power Del.*, vol. 14, no. 3, pp. 1052–1061, Jul. 1999.
[21] R. X. Zeng and J. H. Sinsky, "Modified rational function modeling technique for high speed circuits," pp. 1951–1954, 2006.
[22] M. H. Richardson and D. L. Formenti, "Parameter estimation from frequency response measurements using rational fraction polynomials," pp. 167–186, 1982.
[23] S. Kirkpatrick, C. D. Gelatt, and M. P. Vecchi, "Optimization by simulated annealing," *Sci.*, vol. 220, p. 671, 1983.
[24] P. B. Johnson and R. Christy, "Optical constants of the noble metals," *Phys. Rev. B*, vol. 6, p. 4370, 1972.
[25] S. Foteinopoulou, J. Vigneron, and C. Vandenbem, "Optical near-field excitations on plasmonic nanoparticle-based structures," *Opt. Exp.*, vol. 15, pp. 4253–4267, 2007.
[26] W. Pernice, F. Payne, and D. Gallagher, "Simulation of metallic nano-structures by using a hybrid FDTD-ADI subgridding method," in *Proc. Int. Conf. Electromag. Adv. Applicat. (ICEAA 2007)*, 2007, pp. 633–636.
[27] J. A. Roden and S. D. Gedney, "Convolutional PML (CPML): An efficient FDTD implementation of the CFS-PML for arbitrary media," *Microw. Opt. Tech. Lett.*, vol. 27, pp. 334–338, 2000.

**Lin Han** was born in Jiaozhou, Shandong, China. He received the B.E. degree in electrical engineering and the M.Sc. degree in radio physics from Shandong University, Jinan, China, in 2004 and 2007, respectively. Currently he is pursuing the Ph.D. degree on optoelectronics in Department of Electrical and Computer Engineering, McMaster University, Hamilton, ON, Canada.

His current research interests include computational electromagnetics, the modeling and design of optical devices.

**Dong Zhou** received the Ph.D. degree in Department of Electrical and Computer Engineering, McMaster University, Hamilton, ON, Canada.

His current research interests include computer-aided design of optical devices.

**Kang Li** (M'09) was born in Jinan, China, in 1962. He received the B.S. and M.S. degrees in electrical engineering from Shandong University in 1984 and 1987, and Ph.D. degree in optical engineering from Shandong University, China, in 2006. He is currently a Professor with the School of Information Science and Engineering, Shandong University, Jinan, China.

His research interests include computational electromagnetics and fiber-optic communications.

**Xun Li** (M'93–SM'04) received the B.S. degree from Shandong University, Jinan, China, in 1982, the M.S. degree from the Wuhan Research Institute of Posts Telecommunications, Wuhan, China, in 1984, and the Ph.D. degree from Beijing Jiaotong University, Beijing, China, in 1988.

In 1988, he joined the faculty of the Institute of Lightwave Technology, Beijing Jiaotong University, where he was a Professor. From 1993 to 1999, he was a Research Assistant Professor with the Department of Electrical and Computer Engineering, University of Waterloo, Waterloo, ON, Canada. In 1999, he joined the Department of Electrical and Computer Engineering, McMaster University, Hamilton, ON, where he is currently a Professor. In China, he was mainly involved in the development of III-V compound semiconductor laser diodes. Since 1993, he has been involved in research in the area of quantum electronics with an emphasis on computer-aided design, modeling and simulation of semiconductor optoelectronic devices, waveguide-based integrated photonic devices, and their applications on optical fiber communication systems and networks. He cofounded Apollo Photonics, Inc., and developed one of the company's major software products "Advanced Laser Diode Simulator." He has authored or coauthored more than 100 journal and conference papers. He is also an Adjunct Professor at Beijing Jiaotong University.

Dr. Li was awarded many times by the Chinese National and Local Governments and by Beijing Jiaotong University. He is a member of the Optical Society of America and the International Society for Optical Engineers. He is a Licensed Professional Engineer of Ontario, Canada.

**Wei-Ping Huang** (M'88–SM'96) received the B.S. degree (with provincial and national honors) in electronics from Shandong University, Jinan, China, in 1982, the M.S. degree in electrical engineering with major in photonics from the University of Science and Technology of China, Hefei, China, in 1984, and the Ph.D. degree in electrical engineering with major in photonics from Massachusetts Institute of Technology (MIT), Cambridge, in 1989.

He was with the University of Waterloo, Waterloo, ON, Canada, where he was an Assistant Professor during 1989, an Associate Professor during 1992, and a Professor during 1996. He was also with Nortel (Canada) and NTT (Japan), and was founded several technology ventures and assumed executive and advisory roles through the various stages of business. He is the leader for a number of research projects sponsored by the Canadian Federal and Ontario provincial governments and private companies in the areas of photonic integrated devices and circuits and fiber-optic communication systems. He is internationally known for his contributions and expertise for photonic devices and integrated circuits, especially in the computer-aided design technologies for photonic devices and ICs. He has authored or coauthored more than 160 journal papers and 100 conference papers, and holds seven U.S. patents.

Dr. Huang is a Fellow of the MIT Electromagnetics Academy. He was elected as a Cheung Kong Scholar by the Ministry of Education, China, and Li Ka Sheng Foundation, Hong Kong, in 2000.